Naples, 13/09/2017

Dear referee #1,
Thanks for your comments and revisions, which we have carefully taken into account.
We tried to improve the clarity of the paper according to your suggestions.
We thank you very much for your consideration and we send you our best regards.
Dr. Diana Di Luccio
Prof. Guido Benassai

Dear referee #2,
throws for the accurate review, which allowed us to improve the readability of the manuscript.
We synthesize the main corrections in the following.
- In the introduction we added some references to similar projects, including the USGS forecasting tool;
- Fig. 1: we added geographical coordinates, the La Spezia SWAM buoy site, mean sea level, mean spring tidal range and position of the structures on the beach;
- We included the Holman (1991) reference for ARGUS shoreline imagery in pag.3 line 11;
- We defined the run-up $Ru_{10\%}$ consistently with the other definitions, following Van der Meer et al. (2016), pag. 3 lines 28-31;
- We added information on beach slope and sediment sampling with relative reference, pag 5 lines 14-16;
- We relocated the sentence in previous pag. 4 lines 3-4;
- We changed Fig. 4 and modified the caption accordingly with your suggest;
- We explained that the beach slope was only measured and not dynamically calculated, pag 9 lines 9-11;
- Section 3.2 was revised, including also Poate et al. (2016) run-up equation and changing the Figs. 13 and 14 and the Tab. 2 and 3;
- We revised the definition of β_f introduced by Stockdon et al. (2006), pag. 10 lines 4-5;
- In section 3.3.1 we referred to Fig. 8, as suggested;
- We explained the acquisition and data processing technique for the images, describing in particular the images rectification and the timestack method, pag. 12 lines 8-13;
- We added the wave storm period information, pag. 16 line 5;
- We revised the paragraph, previous pag. 14 lines 4-8;
- We added more comments in the discussion. In particular, we discussed the offshore validation results, accordingly to the different space and time scale of the simulated and observed data; moreover, for the run-up validation results, we added the Fig. 9, which allowed us to discuss the behaviour of the run-up equations in different slopes and different wave conditions;
- We expanded the conclusion;
- Finally we added the section 4.2 in order to evidence the sensitivity of the different run-up equations to the beach slope and wave characteristics.

We thank you very much for your consideration and we send you our best regards.
Dr. Diana Di Luccio
Prof. Guido Benassai

Wave run-up prediction and observation in a micro-tidal beach

Diana Di Luccio[1], Guido Benassai[2], Giorgio Budillon[1], Luigi Mucerino[3], Raffaele Montella[1], and Eugenio Pugliese Carratelli[4]

[1]University of Naples "Parthenope", Science and Technologies Department, Centro Direzionale Is. C4, 80143 Napoli, Italy
[2]University of Naples "Parthenope", Engineering Department, Centro Direzionale Is. C4, 80143 Napoli, Italy
[3]University of Genova, Department of Earth, Environment and Life Sciences, Corso Europa 26, 16132 Genova, Italy
[4]Inter-University Consortium for the Prediction and Prevention of Major Risks Hazards (CUGRI), 84080 Penta di Fisciano (SA), Italy

Correspondence to: Diana Di Luccio (diana.diluccio@uniparthenope.it)

Abstract. Extreme weather events have significant impacts on coastal human activities and related economy. In this scenario, the forecast of sea storms and wave run-up events, in order to mitigate the effects of waves on shores, piers and coastal structures, is a challenging goal. To this end, we used a computational model chain based on both community and ad-hoc developed numerical calculator to evaluate the wave run-up levels, and compared the results of simulated and observed wave run-up levels on a micro-tidal beach located on the Ligurian Sea. The offshore wave simulations were performed by a version of WaveWatch III model, implemented by Campania Center for Marine and Atmospheric Monitoring and Modelling (CCMMMA) - University of Naples "Parthenope", which were used as initial conditions for run-up calculations using different empirical formulas; the validation of the simulated wave characteristics was performed using different observation systems, remote sensing data for offshore waves and observations taken from a video camera system for the run-up levels. We analyze the agreement of the run-up $Ru_{2\%}$ formulas with the observed values, through statistical errors in order to measure the capability of the modelling system to properly simulate the beach run-up during a storm.

The results of this validation study are that some formulas, in agreement with the recent literature, depend on the wave storm intensity, so these empirical run-up formulas, used in coastal vulnerability context, have to be managed with caution, particularly on gravel beaches.

Keywords: model chain, wave numerical model, beach run-up, video monitoring.

1 Introduction

The monitoring and forecasting of wind-wave interaction processes become particularly critical along coastal areas, which are highly dynamic complex systems that respond in a nonlinear manner to external perturbations, giving rise to coastal vulnerability (Didenkulova, 2010; Di Paola et al., 2014), and coastal risk due to sea-level rise (Benassai et al., 2015a) and subsidence (Aucelli et al., 2016). Based on these premises, the evolution of winds, waves and the wind-driven sea circulation is of great applicative relevance for both the modelling and the forecasting of the wave climate (Bertotti and Cavaleri, 2009; Cavaleri and Rizzoli, 1981; Mentaschi et al., 2013; Benassai and Ascione, 2006a) and the observation of oceanographic phenomena (Bidlot et al., 2002). However, coastal areas are critical to monitor both from in-situ and remote sensing perspective. In fact, satellite
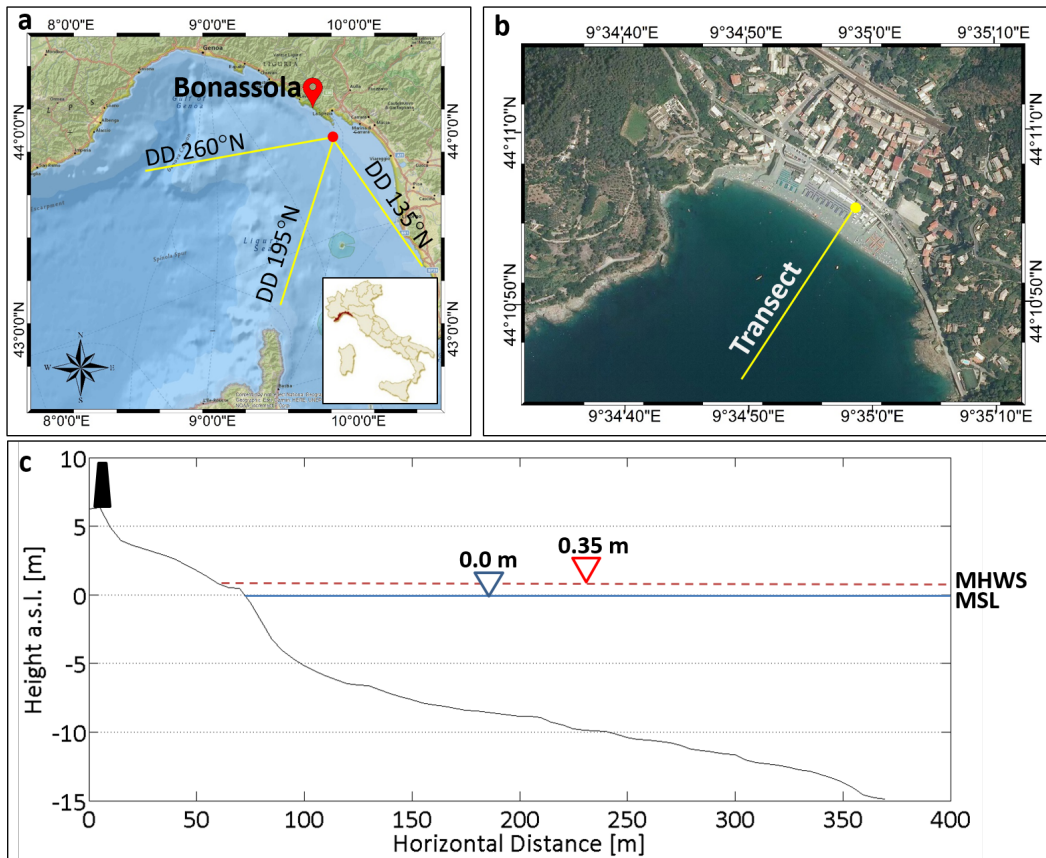
Figure 1. Bonassola beach study area with (a) the location of La Spezia SWAN buoy (red circle) and the main and secondary fetches (Image Source: National Geographic); (b) the monitored cross-shore transect with video-camera system location (yellow circle), (image source: http://www.pcn.minambiente.it/mattm/servizio-wms/); (c) the beach profile along the transect with the location of the anthropic structures (black trapezium), mean sea level (MSL) and the mean spring tidal range (MHSW) were extracted by the official Italian tide archives(http://www.mereografico.it).

data do not reach the adequate resolution and quality when approaching the coast (Aulicino et al., 2018; Cotroneo et al., 2016) while in situ oceanographic data collection is expensive if performed through classical oceanographic cruises or suffers of limitations due to marine traffic or social impact when performed through unmanned maritime vehicle (UMV) (Aulicino et al., 2016). The wind-wave simulations critically depend on the quality of the driving wind fields (Rusu et al., 2014), which are provided by forecasting and/or climatological winds or alternatively by active satellite-based microwave Synthetic Aperture Radar (SAR) (Johannessen and Bjorgo, 2000). The comparison between the wave simulations obtained by these different data sources has demonstrated the capability of the SAR-based wind field retrieval to improve coastal wind-wave modelling (Benassai et al., 2013a, b, 2015b, 2018). With regard to coastal zone monitoring, Lippmann and Holman (1989) were the first to link the bands of white in time exposure images to the crest position of underlying sand bars. The coastline can be surveyed by remote sensing acquisition (Nunziata et al., 2016), UAV (Benassai et al., 2017) and video monitoring (Brignone et al., 2012), which has first been used to investigate also sub-aerial beach topography (Holman et al., 1991).

In particular, wave run-up prediction is required in most coastal vulnerability and risk evaluation projects (Didenkulova and Pelinovsky, 2008; Didenkulova et al., 2010). Wave run-up is defined as "the landward extent of wave uprush measured vertically from the still water level" (Melby et al., 2012). The earliest formulation of run-up height was provided in Hunt (1959) who calculated run-up from incident regular waves. He gave the following equation:

$$\frac{Ru}{H_0} = \xi \tag{1}$$

where ξ is the Iribarren number or surf similarity parameter (Battjes, 1975)

$$\xi = \frac{tan\beta}{\sqrt{\frac{H_0}{L_0}}} \tag{2}$$

and β is the beach slope angle, H_0 is the deep water significant wave height and L_0 is the linear theory deep-water wavelength (Airy, 1841)

$$L_0 = \frac{gT^2}{2\pi} \tag{3}$$

where T is the wave period.

Although a number of available numerical models (Dodd, 1998; Hubbard and Dodd, 2002) give accurate estimates of wave run-up for given boundary conditions, simplified run-up formulas are useful to give realistic results on existing cross-shore profiles.

Holman (1986) measured extreme value statistics for shoreline maxima from a single beach and correlated them with the offshore Irribarren number. Mase (1989) performed an extensive series of laboratory tests for the prediction of run-up elevations of random waves on gentle smooth and impermeable slopes as a function of surf similarity parameter. He included irregular waves and statistical values of the obtained run-up levels, that is Ru_{max} (the highest run-up elevation), $Ru_{2\%}$ (the run-up elevation which is exceeded by 2%), $Ru_{10\%}$ (the run-up elevation which is exceeded by 10%), $Ru_{33\%}$ (the run-up elevation which is exceeded by 33%), Ru_{mean} (the average of the total run-up elevation) (van der Meer et al., 2016). He also introduced two

coefficients which are dependent on the characteristic run-up level $Ru_{x\%}$, as defined in section 3.2.

Stockdon et al. (2006) extended the work of Holman (1986) to several beaches covering a wide range of offshore wave conditions to derive a parametric predictor of the total run-up height. They considered the run-up level $Ru_{2\%}$ as a function of the two different contributions of wave set-up and swash.

5 Poate et al. (2016) demonstrated that wave run-up on gravel beaches under energetic wave conditions was significantly under predicted by the Stockdon et al. (2006) equation and proposed a new run-up parameterization to (pure) gravel beaches. They explained that on sandy beaches under extreme wave, run-up conditions becomes dominated by infragravity waves (Guza and Thornton, 1982; Senechal et al., 2011) with the incident storm waves breaking and dissipating their energy further offshore, whereas on gravel beaches very large waves can impact directly on the beach.

10 One of the main impediments to making valid run-up predictions was the difficulty of obtaining observations of run-up on a wide range of storm wave conditions. This limitation was overcome by video recordings of run-up, performed, among others, by Ruggiero et al. (2004), Bryan and Coco (2007) who collected vertical run-up elevation time series using the "timestack" method (Aagaard and Holm, 1989; Holland and Holman, 1993). Since then, a number of run-up measurements using remote video imagery of the beach were performed.

15 Following Stockdon et al. (2007) wave run-up elevation and setup were calculated from modeled offshore wave conditions using SWAN (Sea WAve measurement Network) and an empirical parameterizations (Stockdon et al., 2006) for the evaluation of coastal vulnerability and run-up elevation. In the last years USGS National Assessment of Coastal Change Hazards project is working in collaboration with the National Oceanic and Atmospheric Administration (NOAA)/National Weather Service (NWS) and the National Centers for Environmental Prediction (NCEP) to make total water level and coastal change

20 forecasts (https://coastal.er.usgs.gov/hurricanes/research/twlviewer/). This operational model combines NOAA wave and water level predictions and a USGS wave run-up model with beach slope observations to provide regional weather offices with detailed forecasts of total water levels (Stockdon et al., 2012; Doran et al., 2015). Following Paprotny et al. (2014), forecasts of wave run-up on two beaches of Polish Baltic Sea coast were tested to evaluate flooding, chaining WAM wave model with run-up empirical formulas, during SatBaltyk Operating System-Shores.

25 In this paper we compute the wave run-up levels with the previous different formulations to obtain run-up time series. Since no local measurements from buoys were available (Montella et al., 2008), a version of WaveWatch III (WW3) model implemented by Campania Center for Marine and Atmospheric Monitoring and Modelling (CCMMMA) - University of Naples "Parthenope", was used, taking full benefits of a high spatial resolution weather-ocean forecasting system with a high performance computing (HPC) system for simulation and open environmental data dissemination (Montella et al., 2007). This

30 deep-water numerical model (Ascione et al., 2006) was coupled with a wave propagation model in shallow water which provided the run-up evaluation on the beach. This model chain was tested on a micro-tidal beach located on the Ligurian Sea, in order to assess the reliability of the wave modelling system, already verified in offshore conditions by means of in-situ and remote sensing techniques (Carratelli et al., 2007; Reale et al., 2014; Benassai and Ascione, 2006b) also for the simulation of the beach processes.

35 *Innovation:* Although, in recent years a number of papers have been published on the offshore validation of numerical simula-
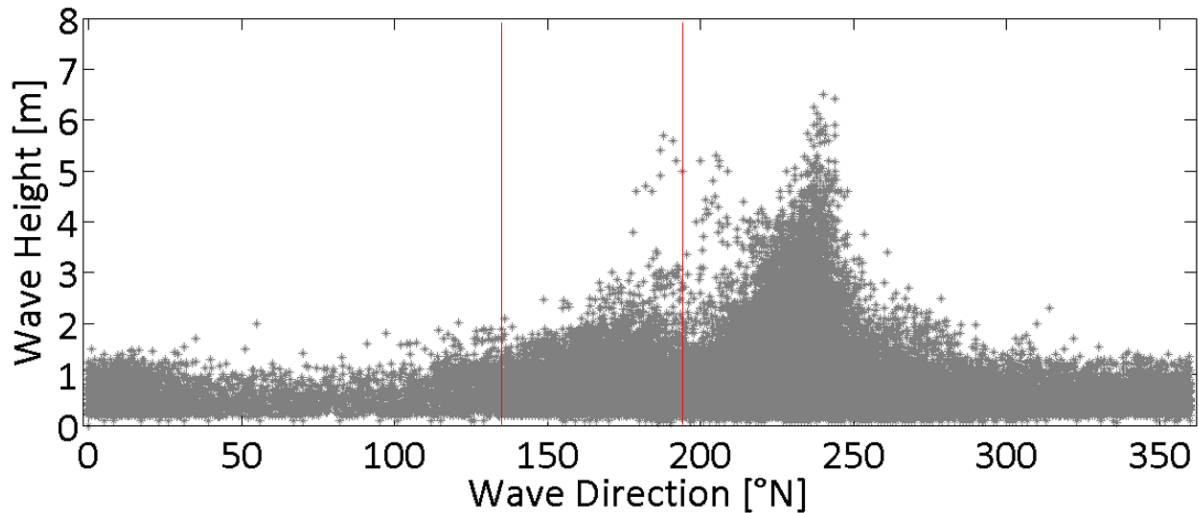
Figure 2. Significant wave heights and wave directions recorded from the SWAN buoy of La Spezia 1989-2009.

tion models, as well as on the nearshore validation of run-up formulas, to the best of our knowledge, very few studies have been published on a global verification of an operational model chain which starts from the forecasted wind till wave and run-up calculation on the beach.

This paper is organized as follows: the field data and the numerical models and the field data are reported in chapter 2 and 3, the results and the comparison with field data are given in chapters 4. Lastly, our discussion and the conclusions are reported in chapter 5 and 6, respectively.

2   Study area and wave climate

The test case presented in this paper was carried out on Bonassola beach (La Spezia, Italy), approx. 410m long, which is located on the eastern coast of Liguria. The coastline is oriented South-East/North-West and it is exposed to waves coming from South-West (215°-245°), while it is protected by the South-East waves. Bonassola beach can be classified as mixed gravel-sand (MSG) beach due to its sediment characteristics and its morphology (Jennings and Shulmeister (2002)). The range of mean sediment grain size in the swash zone is 0.76mm to 62.65mm (0.38 to -5.96 ϕ). The mean beach slope is approximately 8.3% from the shoreline to 10m water depth and becomes 5.5% between 10m and 30m (Fig. 1c). The offshore beach is composed by mean and coarse sand. Information about the grain size and slope of the beach was taken by an analysis conducted by University of Genova in 2012 and documented in Balduzzi et al. (2014).

In order to analyze the extreme sea events, the offshore wave climate was extracted using the data recorded by Italian SWAN buoy located offshore La Spezia (43°55'41.99"N 09°49'36.01"E) since year 1989 till 2009. The directions 195°N and 260°N limit the main fetch, while the directions 135°N and 195°N limit the secondary fetch (in the following S_1). The main transverse sector was later subdivided into two sub-sectors, 195-225°N (S_2) and 225-260°N (S_3), in which two
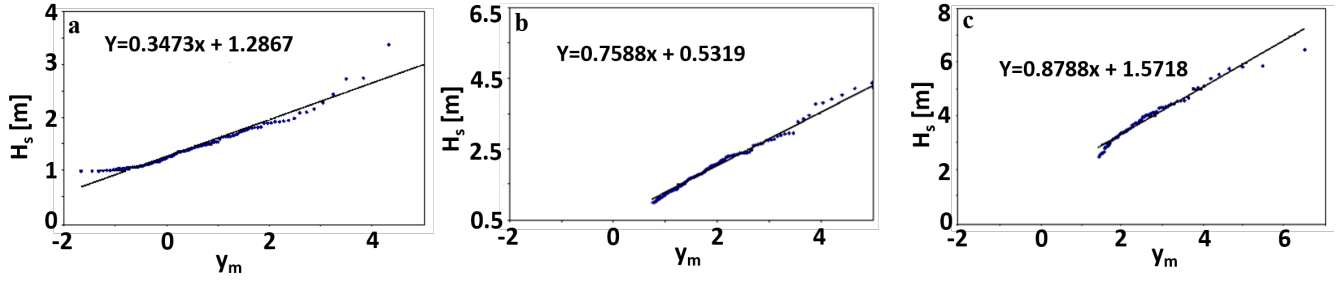
Figure 3. Matching between the recorded extreme wave heights and the reduced variable for Gumbel distribution function for waves coming from a) 135°N-195°N; b) 195°N-225°N; c) 225°N-260°N.

different wave conditions were observed: maximum H_s lower than 5.5m between 195°N and 225°N and higher than 5.5m between 225°N and 260°N (Fig. 2). The H_s time series was processed to obtain the extreme sea storm events. In order to obtain a statistically significant time series, a representative sample of statistically independent extreme wave events N was selected on the basis of the Peak Over Threshold method (Goda, 1989). The 48h-maxima based on over-threshold H^* time series has been sorted in order to find the best fit between the data and the Gumbel (Fisher-Tippet I) cumulative probability distribution function.

$$P(H) = e^{-e^{-\left(\frac{H-B}{A}\right)}} \tag{4}$$

where A is the location parameter and B is the scale parameter. A rank index m, ranging from 1 to N was associated to order the array and the sample rate of non-exceedance $F(H_s < H^*)$ was calculated as

$$F(H_s) < H^* = 1 - \frac{m - 0.44}{N + 0.12} \tag{5}$$

and it is assumed coincident with the non exceedance probability.

$$y_m = -ln[-lnF(H_s < H^*)] \tag{6}$$

Figure 3 shows the rate between $H_s < H^*$ and relative reduced variable for waves coming from each directional sector.

The linear regression line $y = ax + b$ is given as

$$H_s = Ay_m + B \tag{7}$$

where A (slope of the regression line) and B (line intercept) coefficients are linked with the probability distribution function. The wave heights for different return periods can be determined by the following expressions:

$$H_r = Ay_r + B \tag{8}$$

where H_r is the significant wave height with return period T_r and the relative reduced variable is

$$y_r = -ln\left[-ln\left(1 - \frac{1}{\lambda T_r}\right)\right] \tag{9}$$

Table 1. Design waves, in terms of H_r associated to different return periods (T_r equal to 1, 5, 10, 20, 50 and 100 years), obtained from La Spezia buoy (1989-2009) for each directional sector (S_1, S_2 and S_3).

T_r [yr]	Sector	H_r [m]	y_r	T_r [yr]	Sector	H_r [m]	y_r
	S_1	2.84	4.46		S_1	3.88	7.46
1	S_2	3.72	4.20	20	S_2	6.00	7.21
	S_3	5.59	4.57		S_3	8.23	7.57
	S_1	3.40	6.08		S_1	4.20	8.38
5	S_2	4.95	5.82	50	S_2	6.70	8.12
	S_3	7.01	6.19		S_3	9.03	8.49
	S_1	3.64	6.77		S_1	4.44	9.07
10	S_2	5.74	6.51	100	S_2	7.22	8.82
	S_3	7.62	6.88		S_3	9.4	9.18

and the sample intensity λ is defined by the ratio between the number of extreme events and the number of years of observation. Table 1 gives the offshore wave heights obtained for each directional sector as functions of the relative return period T_r, which are maximum for the western directions (sector S_3), with $H_s > 5.0$m.

In order to evaluate the wave run-up levels associated with frequent wave conditions, we selected a recent wave storm coming
5   from a western direction with significant wave heights that can occur several times a year (that is with a return period less than 1 year). We performed numerical simulations on this storm using the WW3 model accompanied by run-up calculations using different empirical formulas.

3 Methods

3.1 Wave numerical simulations

10   The weather/sea forecasting tool in Fig. 4, implemented by CCMMMA was configured using an HPC infrastructure to manage and run a modeling system based on the algorithms implemented in the open-source numerical models Weather Research and Forecasting (WRF) (Skamarock et al., 2001) and WaveWatch III (WW3) (Tolman et al., 2009) organized in a workflow. The present operational system is based on complex data acquisition, processing, simulation, post-processing and inter-comparison dataflow, provided by FACE-IT workflow engine (Pham et al., 2012), available as open source and cloud service. This inte-
15   grated data processing and simulation framework enables: i) the data ingest from geospatial archives; ii) the data regridding, aggregation, and other processing prior to simulation; iii) the leveraging of the high-performance and cloud computing; iv) the post-processing to produce aggregated yields and ensemble variables needed for statistics and model testing. The main workflow tool is the WRF numerical model which gives the 10m wind fields and other atmospheric forcing needed to drive the WW3 model to estimate the offshore waves, which is the initial and boundary conditions for the modeling of waves in shallow
20   water and run-up/overtopping calculator software.
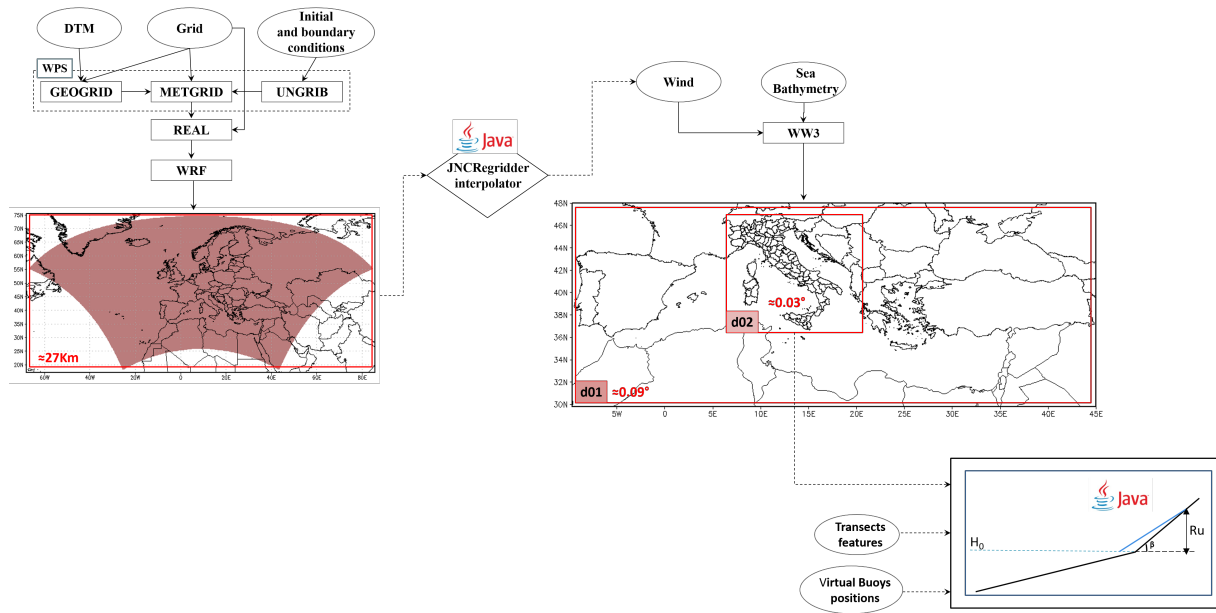
Figure 4. Model chain from the atmospheric model WRF (upper left graphic) to the offshore wave model WW3 (upper right graphic) and the run-up calculator (lower right graphic). The block diagram evidence the input/output components of the model coupling data flux.

Wave simulations were carried out using the WW3 model version 3.14, a third generation wave model developed at NOAA/NCEP. The physics packages used in the our implementation are:

– Linear input parametrization of Cavaleri and Rizzoli (1981) with a filter for low-frequency energy as introduced by Tolman (1992). Source term package of Tolman and Chalikov (1996) have been implemented with stability correction;

5 – Discrete interaction approximation (DIA) (Hasselmann and Hasselmann, 1985) for non-linear wave-wave interactions;

– ULTIMATE QUICKEST propagation scheme (Leonard, 1979) with averaging technique for Garden Sprinkler alleviation Tolman (2002);

– JONSWAP bottom friction formulation (Hasselmann, 1973) with no bottom scattering and Battjes and Janssen (1978) shallow water depth breaking with a Miche-style limiter.

10   In order to produce the numerical simulations presented in this paper, we configured the WW3 model with two one way nested computational domains:

– **Coarse domain**: the domain d01 covers almost the whole Mediterranean Sea by a grid of 608x203 points spaced by a $0.09°$ resolution ($Lon_{min}=9.65°W$, $Lon_{max}=44.98°E$; $Lat_{min}=29.78°N$, $Lat_{max}=47.96°N$)

– **Fine domain**: the d02 domain covers the seas around the Italian peninsula by a grid of 486x353 points spaced by a $0.03°$
15   resolution ($Lon_{min}=6.33°E$, $Lon_{max}=20.88°E$

; $Lat_{min}=36.42°N$, $Lat_{max}=46.98°N$).

Using this configuration we avoided the duty of providing boundary conditions on the south and west boundaries of the d02 domain and considered the d01 as a closed domain forced only by the weather conditions provided by the WRF offline coupled. Outputs from the model include gridded fields with the associated significant wave height (H_s), wave direction (Dir_{mn}), mean period (T_m) and spectral information. The WW3 grid points close to the coast were used as "virtual buoys" (VB) to compute the wave transformation down to the coast, with the final goal of simulating the run-up parameter on the beaches.

3.2 Wave run-up calculator

The last software component of the coupled model chain reported in Fig. 4 (lower right graphic) is the wave run-up calculator on the beach. We used a one-dimensional approach to simulate the beach run-up with a Java software designed to be highly modular as a part of the operational forecasting system. The wave condition in the VB (H_s, T_m and Dir_{mn}) and the beach slope β or β_f derived from a cross-shore beach profile (for example the one shown in Fig. 1), represents the inputs to resolve the run-up empirical equations.

Dealing with random waves, $Ru_{x\%}$ is defined as the wave run-up level, measured vertically from the still water line, which is exceed by $x\%$ of the number of incident waves (van der Meer et al., 2016).

Holman (1986) proposed an empirical formula to obtain $Ru_{2\%}$, based on Iribarren number ξ_f constrained with surf zone slope angle:

$$\frac{Ru_{2\%}}{H_0} = 0.83\xi_f + 0.2 \tag{10}$$

In detail, H_0 depends on the relation between the virtual buoy (VB) ($C_{VB}=L_{VB}/T_m$) and the deep water ($C_0=L_0/T_m$) (Shore Protection Manual, 1984) wave celerity:

$$H_0 = H_s \frac{C_{VB}}{C_0} \tag{11}$$

In VB the wavelength is equal to $L_{VB}=(2\pi)/k$ in which k is the wavenumber obtained by the Hunt approximation of the standard dispersion relation (Fenton and McKee, 1990):

$$(kd)^2 = \left(\frac{\sigma^2 d}{g}\right)^2 + \frac{\left(\frac{\sigma^2 d}{g}\right)}{1 + \sum_{n=1}^{\infty} d_n \left(\frac{\sigma^2 d}{g}\right)^n} \tag{12}$$

where d_n are six constant values given by Fenton and McKee (1990), and σ is the wave frequency.

Mase (1989) on the basis of laboratory tests obtained by the characteristic run-up level $Ru_{x\%}$ as a foundation of two empirical coefficients a and b.

$$\frac{Ru_{x\%}}{H_0} = a\xi^b \tag{13}$$

Mase (1989) suggested a=1.86 and b=0.71 for $Ru_{2\%}$, a=2.32 and b=0.77 for Ru_{max}, a=1.70 and b=0.71 for $Ru_{10\%}$, a=1.38 and b=0.70 for $Ru_{33\%}$, a=0.88 and b=0.69 to obtain Ru_{mean}.

Stockdon et al. (2006) considered the run-up $Ru_{2\%}$ as a function of two separate terms to consider the different contributions of the wave setup and swash (the second term on the left hand side)

$$Ru_{2\%} = 1.1 \left(0.35 \tan \beta_f \left(H_0 L_0 \right)^{0.5} + \frac{\left[H_0 L_0 \left(0.563 \tan \beta_f^2 + 0.004 \right) \right]^{0.5}}{2} \right) \tag{14}$$

where β_f is the average slope over a region $\pm 2\sigma$ around $<\eta>$, where σ is the standard deviation of the continuous water level record, $\eta(t)$. In random waves, H_0 is substituted with the spectral wave height $H_{m0}=4(m_0)^{0.5}$, defined as the incident significant wave height in shallow water, where m_0 is the zero$^{\text{th}}$ spectral moment.

Poate et al. (2016) proposed the following equation, specifically developed for gravel beaches:

$$Ru_{2\%} = C \tan \beta^{0.5} T_m H_s \tag{15}$$

where C is a constant fixed to 0.49 by the Authors.

The mean beach slope β and the foreshore beach slope β_f, used in the run-up equations are calculated taking into account the examined cross-shore beach profile. The equation 14 has been used by a number of researchers to compute coastal inundation and consequently coastal vulnerability and risk (Di Paola et al., 2014; Benassai et al., 2015a). Melby et al. (2012) compared the skill of some different run-up models through some statistical measures and introduced a new statistical skill measure, described in section 3.3.2, which was used to compare different formulations for an extensive dataset. In the following, we compared the skill of different run-up equations through the departure from the observed run-up levels evaluated with video camera records. Among the different empirical formulas used to calculate the wave run-up parameters, the equations (10), (13), (14), (15) have been used to obtain run-up time series. In particular, Holman (1986), Mase (1989), Stockdon et al. (2006) and Poate et al. (2016) formulas have been used for the 2% wave run-up levels, while only Mase (1989) equation has been used to calculate the 10%, 33%, mean and max run-up levels.

3.3 Observations of offshore waves and beach run-up

3.3.1 Altimeter and video monitoring

The validation of the wave model, in terms of offshore wave height, was evaluated against remotely sensed data. The results of this comparison are reported in Fig. 8.

The altimeter footprint along the satellite tracks provides a large spatial coverage over the entire region of the Central and Northern Tyrrhenian Sea, which cannot be accomplished by in-situ observations at fixed stations. The altimeter data was obtained from the dataset of the Ocean Surface Topography Mission (OSTM/Jason-2), launched on 20 June 2008. In this case, we used the Geophysical Data Record (GDR) with spatial resolution of 11.2km (Along) x 5.1km (Across). Fig. 5 shows the considered track of the OSTM/Jason2 satellite.

The beach run-up simulations using the different equations were validated by means of a video monitoring system placed in the middle of Bonassola beach (Fig. 6a,b,c,d). Video recordings of run-up were made using three video cameras, installed
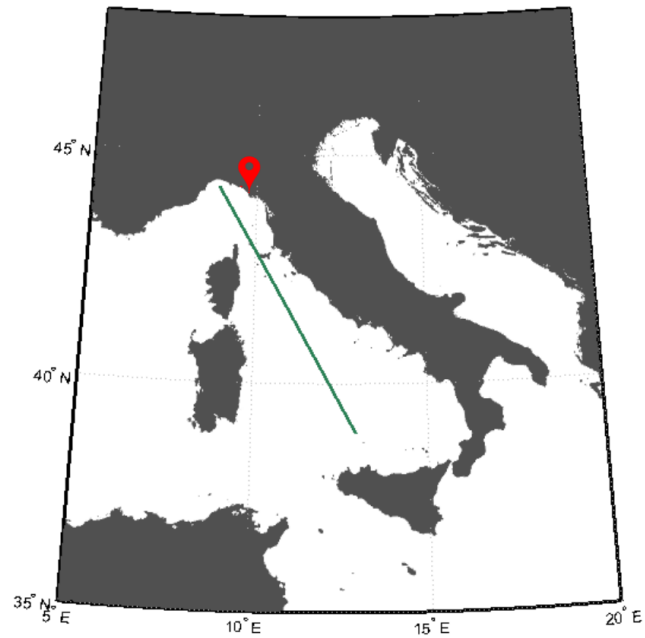
Figure 5. Map showing the position of the dataset to models testing. The green line depicts the OSTM/Jason-2 satellite dataset.
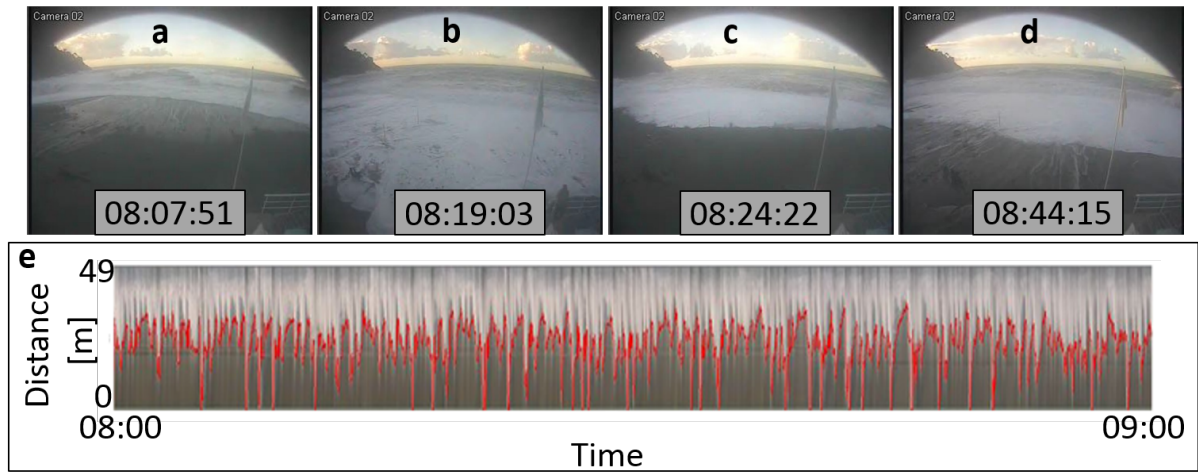
Figure 6. A time sequence (a) (b) (c) (d) of the Bonassola beach sea storm on 10 February 2016; (e) time-stack relative to 10 February 2016 between 08:00-09:00.

at an elevation of about 13m above Mean Sea Level (MSL), which have allowed a complete coverage of the beach since 19 November 2015 to date. Using the geometric transformation between ground and image coordinates, the light intensity of each pixel in the cross-shore transects was digitized. Vertical run-up elevation time series were extracted from video recordings using the time-stack method (Aagaard and Holm, 1989; Holland and Holman, 1997). This methodology, giving rise to the signal

5   reported in Fig. 6e, is described in the extensive literature on coastal video monitoring (Takewaka and Nakamura, 2001; Ojeda et al., 2008; Zhang and Zhang, 2008). The run-up position at each video sample time (1Hz) was obtained with Beachkeeper plus (Brignone et al., 2012), a software based on Matlab algorithm used to analyze the images without any a-priory information of the acquisition system. Run-up results have been validated through camera images geo-rectification, which was performed by using 9 Ground control Points (GCPs).The X-Y coordinates of GCPs were acquired in UTM32-WGS84 using DGPS,

10 with 0.15 meters accuracy on horizontal and vertical positions. The cross-shore resolution of the processed timestack images is 0.2 m, equal to the minimum pixel footprint along the monitored transect, in accordance with (Vousdoukas et al., 2012) and (Huisman et al., 2011). Best results have been processed with 5 pixel lines analysis, reducing backwash detection and filtration/extra-filtration detection, using timestack method.

3.3.2   Comparison statistics

15 The quality of the results provided by the offshore wave model and by the run-up simulations was evaluated by the comparison with wave altimeter records and video-camera run-up observations. Deviation of simulated parameters from observed data was estimated through some of the following statistical error indicators proposed by Mentaschi et al. (2013) (S_i indicate a simulated variable, O_i indicate an observed variable and N is the number of considered observations):

– normalized Bias (BI):

$$BI = \frac{\sum_{i=1}^{N}(S_i - O_i)}{\sum_{i=1}^{N} O_i} \tag{16}$$

– root mean square error (RMSE):

$$RMSE = \sqrt{\frac{\sum_{i=1}^{N}(S_i - O_i)^2}{N}} \tag{17}$$

– normalized root mean square error (NRMSE):

$$NRMSE = \sqrt{\frac{\sum_{i=1}^{N}(S_i - O_i)^2}{\sum_{i=1}^{N} O_i^2}} \tag{18}$$

25 – normalized scatter index (SI):

$$SI = \sqrt{\frac{\sum_{i=1}^{N}[(S_i - \bar{S}) - (O_i - \bar{O})]^2}{\sum_{i=1}^{N} O_i^2}} \tag{19}$$

- linear correlation coefficient (R):

$$R = \frac{cov(S_i, O_i)}{var(O_i) var(S_i)} \tag{20}$$

The results are summarized in the Summary Performance Score (SPS) index, based on the RMSE, BI and SI performance, normalized between 0 and 1 (as suggested by Melby et al. (2012)).

5 – NRMSE Performance (NRMSE$_P$)

$$NRMSE_P = 1 - NRMSE \tag{21}$$

- BI Performance (BI$_P$)

$$BI_P = 1 - |BI| \tag{22}$$

- SI Performance (SI$_P$)

10 $$SI_P = 1 - SI \tag{23}$$

- Summary Performance Score (SPS)

$$SPS = \frac{NRMSE_P + BI_P + SI_P}{3} \tag{24}$$

4 Experimental results

In this section some experimental results are presented and discussed to show the capability and accuracy of wind-wave
15 modelling chain in estimating run-up levels on the beach studied.

4.1 Offshore wave validation with altimeter data

The consistency of the WW3 model was validated taking full benefit of the ku-based altimeter data from OSTM/Jason2 mission, relative to the passage of the satellite during the period from February 9th 2016 at 04:58:44 UTC to 09th 2016 at 05:00:43 UTC. Figs. 7a,b,c depict the simulated WW3 H_s maps on February 10th 2016 at 00:00, 06:00 and 12:00 UTC, with relative zoom, in
20 Figs. 7d,e,f, respectively, while Fig. 8 shows the time history of the measured and modelled offshore H_s along the track.

The results of the wind-wave modelling system were interpolated in both space and time to collocate with the altimeter data. Firstly, hourly WW3 H_s outputs are first spatially interpolated (bilinear interpolation) from the grid points to the locations of the altimeter measurements. Interpolations are then carried out in time to fit the satellite pass (linear time interpolation between the previous and following field values). The observed H_s is shown as a blue line in Fig. 8a, while the simulated H_s is reported
25 as a red line. In general, the model fits the measurements quite well, but sometimes it deviates from the observations. For example, the first high wave event between 41.5°N and 42°N is underestimated by the model, while the second high wave
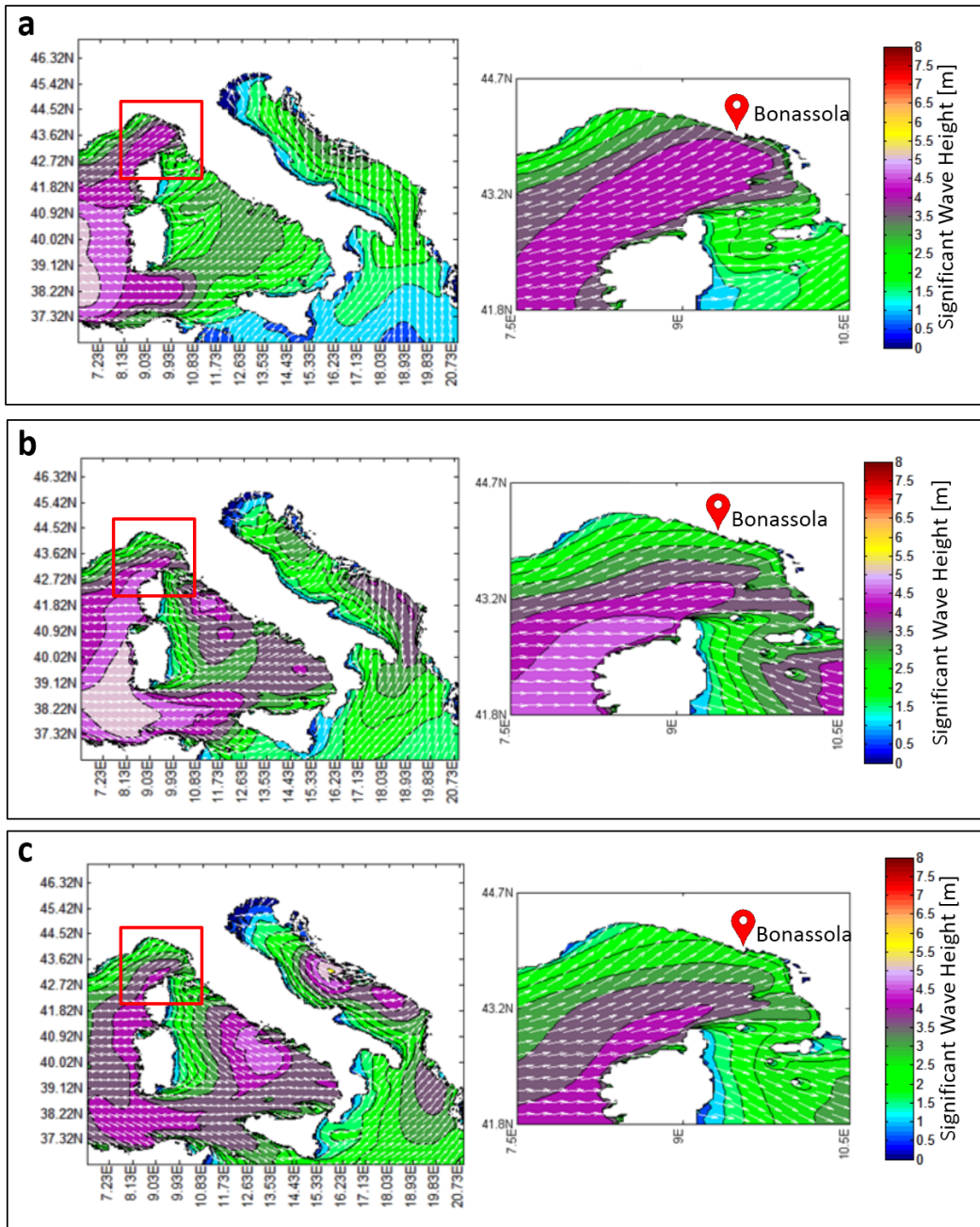
Figure 7. Ligurian Sea significant wave height (color maps) and direction (vector fields) in three moments of sea storm in February 2016. The maps are relative to WW3 model forecast on February 10th 2016 at: (a) 00:00 UTM; (b) 06:00 UTM; (c) 12:00. Wave height isolines are at 0.5m intervals.
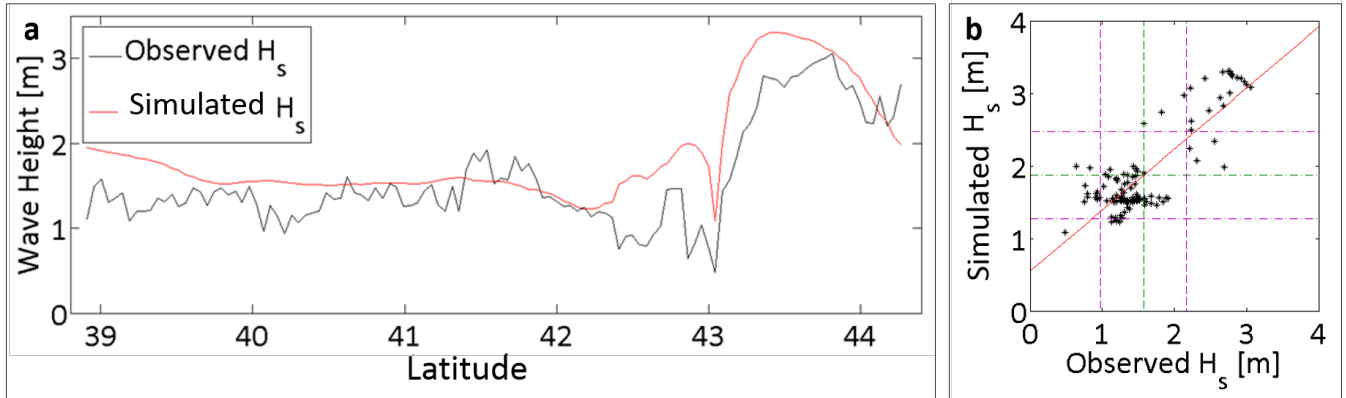
Figure 8. Matching between WW3 and Ku-band altimeter data from JASON-2 satellite pass. 44 cycle 280. (a) Time series during the period from February 9th 2016 at 04:58:44 to 09th 2016 at 05:00:43. (b) Scatter diagram between observed and simulated H_s [m]. The green dotted lines are the mean in x (1.876) and y (1.574) directions, while the purple dotted lines are the relative standard deviation of 0.6022 and 0.5975, respectively.

event between 43.5°N and 44°N is slightly overestimated.

It can also be observed that the simulated H_s trace along the satellite track is much smoother than the observations, due to the fact that the WW3 model is incapable to resolve the small scales seen in the altimeter observations. The statistics of the comparison give an R value of 0.838, a BI of 0.192, a SI of 0.202 and a RMSE value of 0.455m. The satisfactory agreement is shown by a RMSE lower than 0.46m and a correlation coefficient higher than 0.83. In fact, Fig. 8 shows a good match between simulations and observations, however non-negligible differences in terms of H_s can be noted, which can be partially explained taking into account the different spatial gridding resolution scale of modeled (WW3) and remotely sensed (Jason-2) wave estimation products.

4.2 Analysis of the existing wave run-up formulas

In Fig. 9 the run-up Ru$_{2\%}$ normalized with H_s has been reported as a function of the Iribarren number for the different equations considered, in a range of the surf similarity parameter corresponding to dissipative and intermediate beaches (ξ<1.0). The values of β_f (used in Holman (1986) and Stockdon et al. (2006) equations) has been obtained as a multiple N (fixed to 2.25 for convenience) of β (used in Mase (1989) and Poate et al. (2016) equations). Firstly, Fig. 9 evidences that Holman (1986) and Stockdon et al. (2006) equations provide a linear dependence on ξ, while Mase (1989) and Poate et al. (2016) exhibit a nonlinear one. Secondly, the results show an increase in run-up levels as beaches become more reflective (increase of ξ). In particular, with regard to the examined wave storm conditions (H_s equal to 2.5m), Stockdon et al. (2006) equation represents a lower bound for the relative run-up for ξ<0.65, while Holman (1986) equation is an upper bound for run-up at least for ξ>0.45. Poate et al. (2016) gives intermediate results for 0.45≤ ξ ≤0.65, and it gives the lowest results for ξ>0.65.
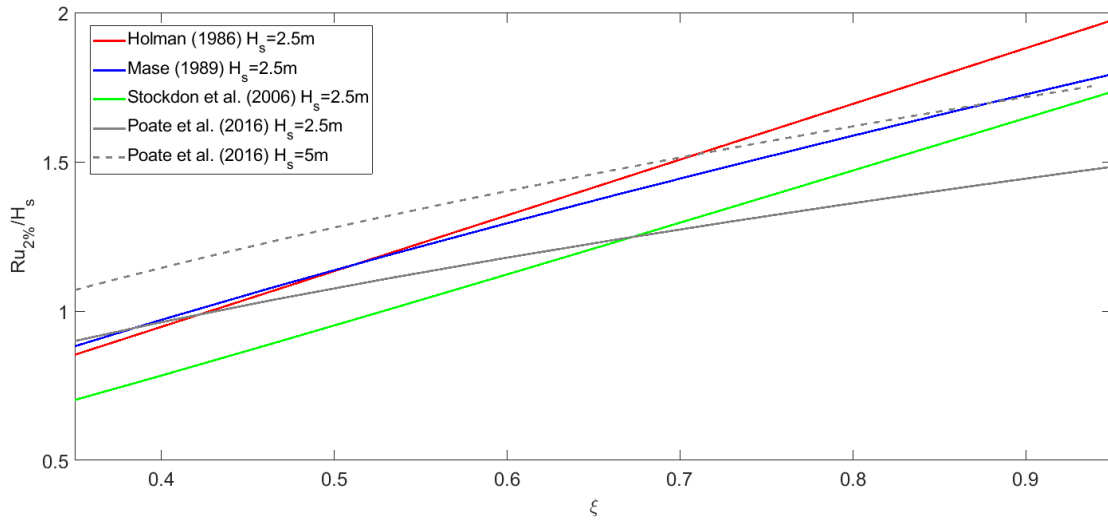
Figure 9. $Ru_{2\%}/H_s$ as a function of Iribarren number ξ for the different equations with reference to the wave conditions of February 2016 storm (H_s=2.5m) and, only for Poate et al. (2016), the same values calculated in more energetic conditions (H_s=2.5m, dotted line)

4.3 Wave run-up simulations and validation with video-monitoring system

In this subsection, wave run-up numerical simulations obtained with the model chain are described with respect to the storm between February 9th and February 11st 2016. A preliminary offshore wave simulation was performed on a virtual buoy located offshore Bonassola beach. The relative H_s and T_m time history is shown in Fig. 10a,b, respectively. The storm exhibited a maximum H_s higher than 3.0m (with relative T_m of about 7s) on February 10th 2016 at 03:00, followed by a decrease of H_s (with relative increase of T_m) in the following hours, with values between 2.0m and 3.0m, in accordance with the regional wave field maps in Fig. 7.

The run-up formulas described in section 3.2 were evaluated considering the wave conditions of February 2016 storm event and the cross-shore transect reported in Fig. ??c. The simulation results have been compared with the observed wave run-up elevation time series recorded by a beach camera system on February 10th 2016 from 08:00am to 16:00pm. Run-up video records (Figs. 11 and 12) were made using the central camera of the video monitoring system described in section 3.3.

The comparison between the different $Ru_{2\%}$ formulas, reported in Fig. 14, shows that the $Ru_{2\%}$ formulas almost always underestimate the levels. In detail, the Holman (1986) results are the highest, followed by Mase (1989), Stockdon et al. (2006) and Poate et al. (2016), in this order. This is consistent with the behaviour of the different formulas evidenced in Fig. 14 for ξ around 0.65, and is confirmed by the RMSE values of 0.41, 0.70, 0.95 and 1.04, respectively, and by the SPS values in decreasing order, 0.92, 0.87, 0.83 and 0.82, respectively. The comparison between the hourly mean of the observed and simulated $Ru_{x\%}$, obtained by Mase (1989) equations, reported in Fig. 14, shows more uniform values of the numerical simulations in the eight hours of analysis, due to the lower time resolution of the WW3 model.

Table 2. $Ru_{x\%}$ observed with cameras versus $Ru_{x\%}$ simulated using different equations.

| | Simulated run-up | | | | | | | | Observed run-up | | | | |
| | Holman (1986) | Mase (1989) | | | | | Stockdon et al. (2006) | Poate et al. (2016) | | | | | |
	$Ru_{2\%}$	$Ru_{2\%}$	$Ru_{10\%}$	$Ru_{33\%}$	Ru_{max}	Ru_{mean}	$Ru_{2\%}$	$Ru_{2\%}$	Ru_{mean}	Ru_{max}	$R_{2\%}$	$R_{10\%}$	$R_{33\%}$
10/02 08-09	3.74	3.46	3.16	2.57	4.22	1.65	3.14	3.07	1.80	4.44	3.92	3.05	2.04
10/02 09-10	3.81	3.52	3.21	2.62	4.30	1.67	3.21	3.13	1.82	3.98	3.63	3.31	2.07
10/02 10-11	3.88	3.58	3.27	2.66	4.38	1.70	3.28	3.21	2.13	4.50	4.36	3.43	2.24
10/02 11-12	3.85	3.53	3.23	2.63	4.33	1.68	3.26	3.17	2.27	4.42	4.10	3.42	2.56
10/02 12-13	3.84	3.49	3.19	2.60	4.29	1.66	3.26	3.13	2.48	4.12	3.95	3.45	2.63
10/02 13-14	3.85	3.48	3.18	2.59	4.28	1.66	3.27	3.13	2.54	4.55	4.33	3.57	2.71
10/02 14-15	4.00	3.63	3.32	2.70	4.46	1.73	3.40	3.29	2.62	4.75	4.52	3.44	2.80
10/02 15-16	4.11	3.76	3.44	2.80	4.62	1.79	3.50	3.44	2.86	5.00	4.80	3.62	2.94

Table 3. Statistical error parameters obtained from the comparison between observed and simulated wave run-up levels.

	R	BI	SI	RMSE	NRMSE	NRMSE$_P$	BI$_P$	SI$_P$	SPS
Holman (1986) Ru$_{2\%}$	0.867	-0.075	0.062	0.410	0.097	0.903	0.925	0.938	0.972
Mase (1989) Ru$_{mean}$	0.424	-0.274	0.157	0.723	0.309	0.691	0.726	0.843	0.753
Mase (1989) Ru$_{33\%}$	0.607	0.059	0.112	0.318	0.126	0.874	0.941	0.888	0.901
Mase (1989) Ru$_{10\%}$	0.576	-0.047	0.039	0.209	0.061	0.939	0.953	0.961	0.951
Mase (1989) Ru$_{2\%}$	0.794	-0.154	0.067	0.704	0.167	0.833	0.846	0.933	0.871
Mase (1989) Ru$_{max}$	0.763	-0.025	0.051	0.255	0.057	0.943	0.975	0.949	0.956
Stockdon et al. (2006) Ru$_{2\%}$	0.871	-0.217	0.063	0.949	0.225	0.225	0.783	0.775	0.832
Poate et al. (2006) Ru$_{2\%}$	0.845	-0.239	0.063	1.039	0.246	0.754	0.761	0.973	0.817
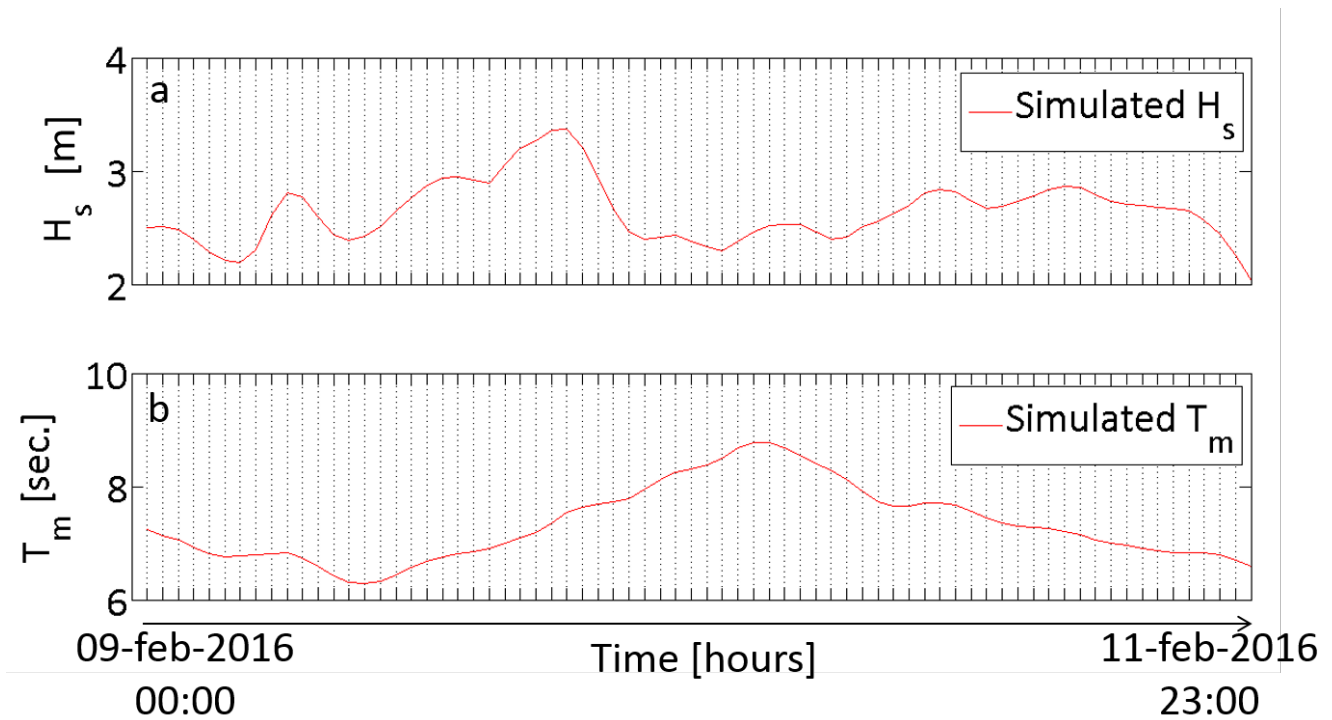
Figure 10. Forecasted significant wave height (H_s) and mean wave period (T_m) relative February 09th-11th 2016 sea storm at virtual buoy near Bonassola beach.

5 Discussion

Firstly, we noted that the validation of the model chain is affected by systematic errors due to spatial and temporal resolution. In fact, the altimeter observations are relative to the track of Fig. 5, which is not coincident with the location of the virtual buoy. This circumstance doesn't allow us to strictly correlate the offshore wave validations with the run-up on the beach.

In particular, the validation results of the offshore wave simulations with respect to the altimeter data showed a satisfactory agreement with a BIAS of 0.192 and a standard deviation (SD) lower than 0.6m. These results slightly overpredict the measured values, in agreement with the ones of Wahle et al. (2017), who compared Saral/Altika altimeter data with the WAM (WAve Model) simulations.

The beach run-up validation is also affected by errors due to camera resolution in time stack mode, equal to 0.2 pixel, and to DGPS accuracy. Moreover, additional discrepancies between run-up simulations and camera observations can bel inked to the time shift between model chain output step (1h) and video recording (1s), which produce smoother simulated run-up results, as already evidenced in Fig. 14.

With regard to the agreement between the different run-up empirical calculations and the observed values, we reported the non dimensional run-up 2% levels as a function of the Iribarren number in Fig. 9. The experimental values, in the ξ range consid-
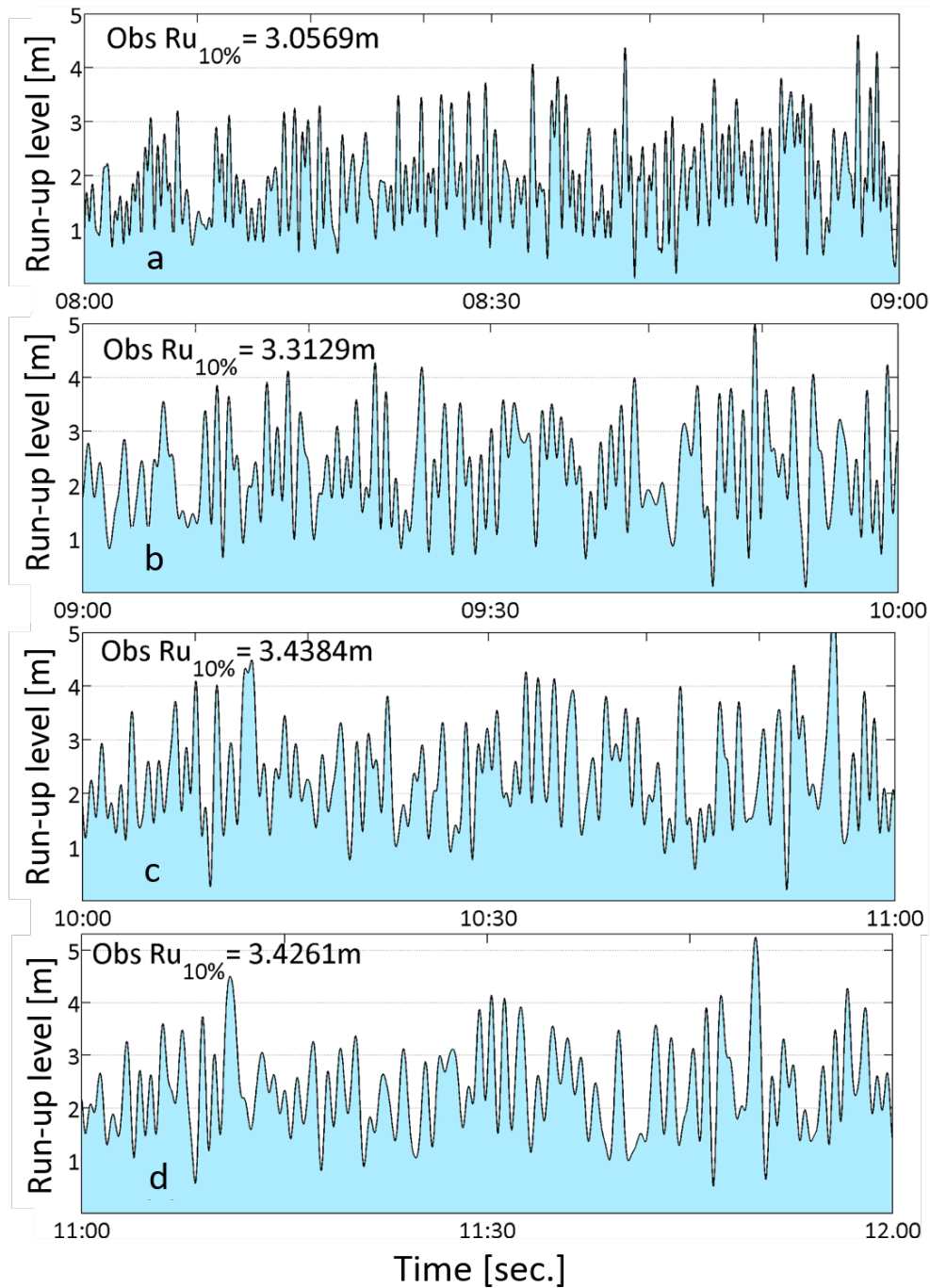
Figure 11. Wave run-up levels collected using pixel time stacks derived from video data of camera at Bonassola on February 10th 2016 at: (a) 8:00-9:00 UTC; (b) 9:00-10:00 UTC; (c) 10:00-11:00 UTC; (d) 11:00-12:00 UTC
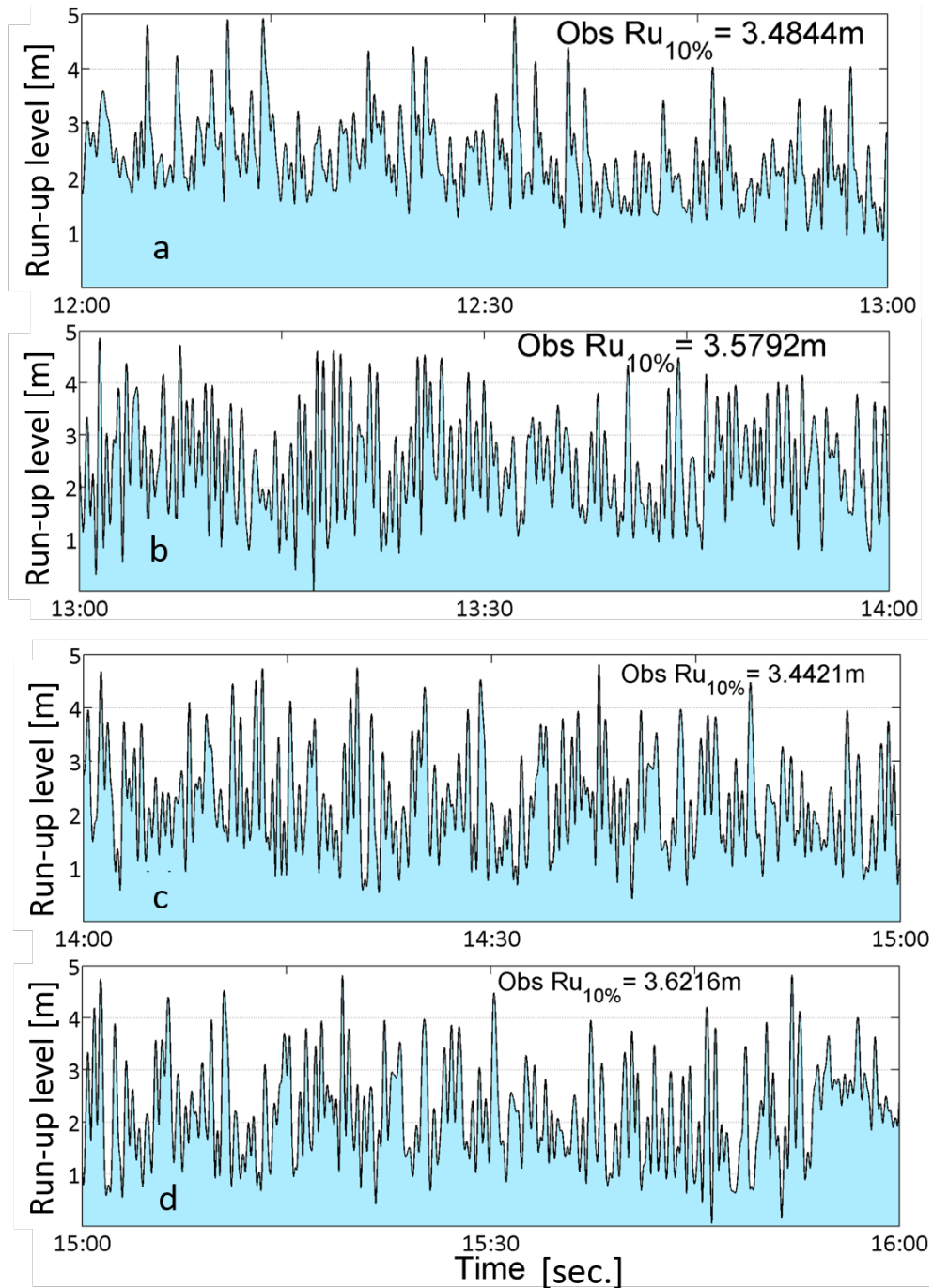
Figure 12. Wave run-up levels collected using pixel time stacks derived from video data of camera at Bonassola on February 10th 2016 at: (a) 12:00-13:00 UTC; (b) 13:00-14:00 UTC; (c) 14:00-15:00 UTC; (d) 15:00-16:00 UTC.
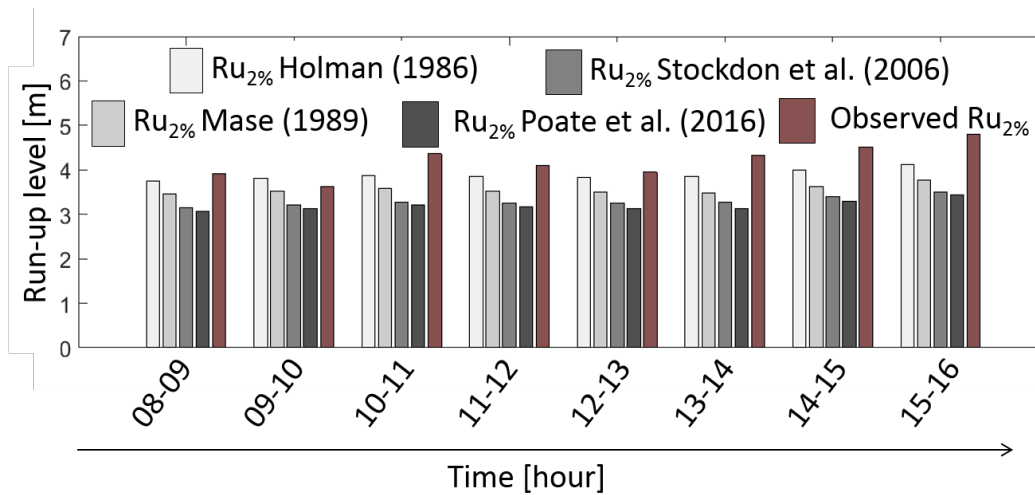
Figure 13. Comparison among observed and simulated $Ru_{2\%}$ with different formulas.
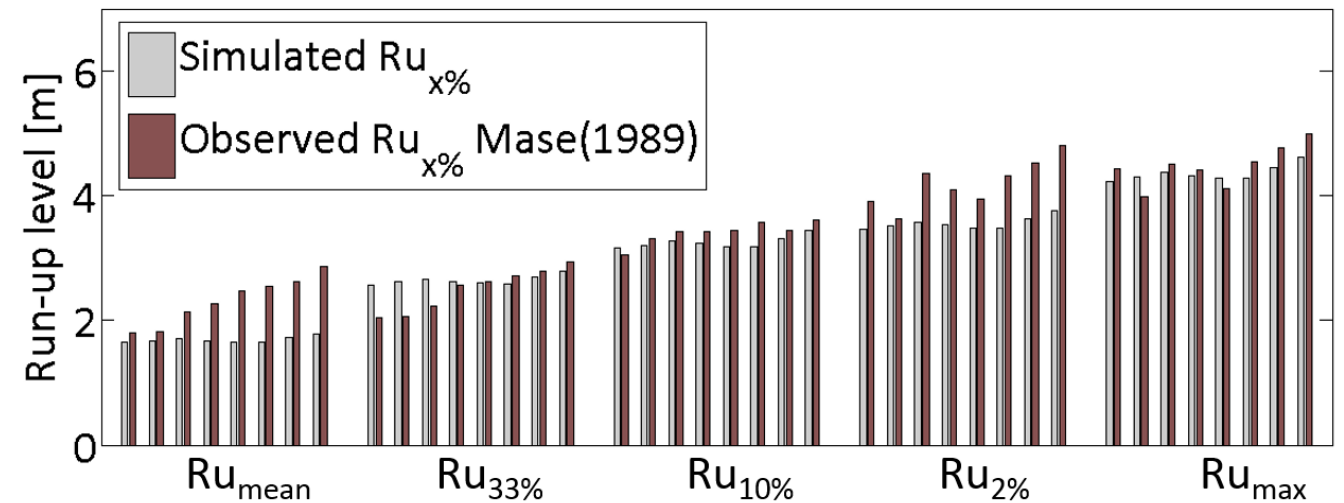
Figure 14. Comparison among different $Ru_{x\%}$ calculated with Mase (1989) equations and observations.

ered, are closer to Holman (1986), Mase (1989), Stockdon et al. (2006) and Poate et al. (2016) in this order, in accordance with their RMSE values, which are 0.41, 0.70, 0.95 and 1.04, respectively. This is also in agreement with SPS values given in Table 3. These results evidence that Stockdon et al. (2006) equation represents a lower bound limit for $Ru_{2\%}$ in the ξ range lower than 0.65. This is consistent with the Poate et al. (2016) considerations, who noted an underestimation of Stockdon et al. (2006)

5   equation, which affected the some Poate et al. (2016) equation for moderate wave conditions. Nevertheless, in more energetic

conditions, the Poate et al. (2016) equation represents an upper bound for run-up, at least in the range $\xi > 0.65$, as it is reported in Fig. 9.

6 Conclusion and future directions

This paper presents the results of a numerical model chain which begins with the European forecasted winds which are downscaled and given as input to an offshore wave model, followed by beach run-up calculator. The model chain has been validated for both offshore and inshore conditions.

The comparison between the simulated and observed results shows that the modelling chain wave run-up simulations in the time domain are reliable for an alert system. Neverthless, the system still presents a number of limits linked, on one hand, to the output time and space resolution and, on the other hand, to the limited range of wave parameter and beach slope considered. In fact, it must be pointed out that the empirical run-up equations are influenced by the wave height level (as reported in Fig. 9) and by the beach slope particularly in the foreshore zone. This considerations stimulate us to extend the field campaign to different wave conditions and different beach grain size sediments.

In the near future, we will increase the spatial and temporal resolution of the model chain in order to enable the run-up calculations for more complex beach configurations. This improvement will need the implementation of the model chain using a cloud computing powered (Montella et al., 2015) GPGPU based approach (Di Lauro et al., 2012) in order to reduce the overall computational costs.

Acknowledgements. The authors are grateful to the CCMMMA (*Campania Center for Marine and Atmospheric Monitoring and Modelling*, http://meteo.uniparthenope.it), that is the forecast service of the University of Napoli "*Parthenope*" for the real time monitoring and forecast of marine, weather and air quality conditions in the Mediterranean area. The CCMMMA provided the hardware and software resources for the offshore numerical simulations.

References

Aagaard, T. and Holm, J.: Digitization of wave run-up using video records, Journal of Coastal Research, pp. 547–551, 1989.

Airy, G. B.: Tides and waves, Encyclopaedia Metropolitana, 3, 1817–1845, 1841.

Ascione, I., Giunta, G., Mariani, P., Montella, R., and Riccio, A.: A grid computing based virtual laboratory for environmental simulations, Euro-Par 2006 Parallel Processing, pp. 1085–1094, 2006.

Aucelli, P. P. C., Di Paola, G., Incontri, P., Rizzo, A., Vilardo, G., Benassai, G., Buonocore, B., and Pappone, G.: Coastal inundation risk assessment due to subsidence and sea level rise in a Mediterranean alluvial plain (Volturno coastal plain–southern Italy), Estuarine, Coastal and Shelf Science, 2016.

Aulicino, G., Cotroneo, Y., Lacava, T., Sileo, G., Fusco, G., Carlon, R., Satriano, V., Pergola, N., Tramutoli, V., and Budillon, G.: Results of the first Wave Glider experiment in the southern Tyrrhenian Sea, Advances in Oceanography and Limnology, 7, 2016.

Aulicino, G., Cotroneo, Y., Ruiz, S., Román, A. S., Pascual, A., Fusco, G., Tintoré, J., and Budillon, G.: Monitoring the Algerian Basin through glider observations, satellite altimetry and numerical simulations along a SARAL/AltiKa track, Journal of Marine Systems, 179, 55–71, 2018.

Balduzzi, I., Cavallo, C., Corredi, N., and Ferrari, M.: L'érosion des plages de poche de la Ligurie: le cas d'étude de Bonassola (La Spezia, Italie), Geo-Eco-Trop, 38, 187–198, 2014.

Battjes, J. A.: Surf similarity, in: Coastal Engineering, Proceedings of 14th Conference on Coastal Engineering, Copenhagen, Denmark, 1974, vol. 14, pp. 466–480, ASCE, 1975.

Battjes, J. A. and Janssen, J.: Energy loss and set-up due to breaking of random waves, in: Coastal Engineering 1978, pp. 569–587, 1978.

Benassai, G. and Ascione, I.: Implementation and validation of wave watch III model offshore the coastlines of Southern Italy, in: Proceedings of 25th International Conference on Offshore Mechanics and Arctic Engineering, pp. 553–560, American Society of Mechanical Engineers, 2006a.

Benassai, G. and Ascione, I.: Implementation of WWIII wave model for the study of risk inundation on the coastlines of Campania, Italy, Environmental Problems in Coastal Regions VI: Including Oil Spill Studies, 88, 249, 2006b.

Benassai, G., Migliaccio, M., and Montuori, A.: Sea wave numerical simulations with COSMO-SkyMed© SAR data, Journal of Coastal Research, 65, 660–665, 2013a.

Benassai, G., Montuori, A., Migliaccio, M., and Nunziata, F.: Sea wave modeling with X-band COSMO-SkyMed© SAR-derived wind field forcing and applications in coastal vulnerability assessment, Ocean Science, 9, 325, 2013b.

Benassai, G., Di Paola, G., and Aucelli, P. P. C.: Coastal risk assessment of a micro-tidal littoral plain in response to sea level rise, Ocean & Coastal Management, 104, 22–35, 2015a.

Benassai, G., Migliaccio, M., and Nunziata, F.: The use of COSMO-SkyMed© SAR data for coastal management, Journal of Marine Science and Technology, 20, 542–550, 2015b.

Benassai, G., Aucelli, P., Budillon, G., De Stefano, M., Di Luccio, D., Di Paola, G., Montella, R., Mucerino, L., Sica, M., and Pennetta, M.: Rip current evidence by hydrodynamic simulations, bathymetric surveys and UAV observation, Natural Hazards and Earth System Sciences, 17, 1493–1503, 2017.

Benassai, G., Di Luccio, D., Corcione, V., Nunziata, F., and Migliaccio, M.: Marine Spatial Planning Using High-Resolution Synthetic Aperture Radar Measurements, IEEE Journal of Oceanic Engineering, 2018.

Bertotti, L. and Cavaleri, L.: Wind and wave predictions in the Adriatic Sea, Journal of Marine Systems, 78, S227–S234, 2009.

Bidlot, J.-R., Holmes, D. J., Wittmann, P. A., Lalbeharry, R., and Chen, H. S.: Intercomparison of the performance of operational ocean wave forecasting systems with buoy data, Weather and Forecasting, 17, 287–310, 2002.

Brignone, M., Schiaffino, C. F., Isla, F. I., and Ferrari, M.: A system for beach video-monitoring: Beachkeeper plus, Computers & Geosciences, 49, 53–61, 2012.

5 Bryan, K. and Coco, G.: Detecting nonlinearity in run-up on a natural beach, Nonlinear Processes in Geophysics, 14, 385, 2007.

Carratelli, E. P., Budillon, G., Dentale, F., Napoli, F., Reale, F., and Spulsi, G.: An experience in monitoring and integrating wind and wave data in the Campania Region, Bollettino di Geofisica Teorica ed Applicata, 48, 215–226, 2007.

Cavaleri, L. and Rizzoli, P. M.: Wind wave prediction in shallow water: Theory and applications, Journal of Geophysical Research: Oceans, 86, 10 961–10 973, 1981.

10 Cotroneo, Y., Aulicino, G., Ruiz, S., Pascual, A., Budillon, G., Fusco, G., and Tintoré, J.: Glider and satellite high resolution monitoring of a mesoscale eddy in the algerian basin: Effects on the mixed layer depth and biochemistry, Journal of Marine Systems, 162, 73–88, 2016.

Di Lauro, R., Giannone, F., Ambrosio, L., and Montella, R.: Virtualizing general purpose GPUs for high performance cloud computing: an application to a fluid simulator, in: Parallel and Distributed Processing with Applications (ISPA), 2012 IEEE 10th International Symposium on, pp. 863–864, IEEE, 2012.

15 Di Paola, G., Aucelli, P. P. C., Benassai, G., and Rodríguez, G.: Coastal vulnerability to wave storms of Sele littoral plain (southern Italy), Natural hazards, 71, 1795–1819, 2014.

Didenkulova, I.: Marine natural hazards in coastal zone: observations, analysis and modelling (Plinius Medal Lecture), in: EGU General Assembly Conference Abstracts, vol. 12, p. 14748, 2010.

Didenkulova, I. and Pelinovsky, E.: Run-up of long waves on a beach: the influence of the incident wave form, Oceanology, 48, 1–6, 2008.

20 Didenkulova, I., Sergeeva, A., Pelinovsky, E., and Gurbatov, S.: Statistical estimates of characteristics of long-wave run-up on a beach, Izvestiya, Atmospheric and Oceanic Physics, 46, 530–532, 2010.

Dodd, N.: Numerical model of wave run-up, overtopping, and regeneration, Journal of Waterway, Port, Coastal, and Ocean Engineering, 124, 73–81, 1998.

Doran, K. S., Long, J. W., and Overbeck, J. R.: A method for determining average beach slope and beach slope variability for US sandy
25 coastlines, Tech. rep., US Geological Survey, 2015.

Fenton, J. D. and McKee, W.: On calculating the lengths of water waves, Coastal Engineering, 14, 499–513, 1990.

Goda, Y.: On the methodology of selecting design wave height, in: Coastal Engineering Proceedings 1988, vol. 21, pp. 899–913, ASCE, 1989.

Guza, R. and Thornton, E. B.: Swash oscillations on a natural beach, Journal of Geophysical Research: Oceans, 87, 483–491, 1982.

30 Hasselmann, K.: Measurements of wind wave growth and swell decay during the Joint North Sea Wave Project (JONSWAP), Dtsch. Hydrogr. Z., 8, 95, 1973.

Hasselmann, S. and Hasselmann, K.: Computations and parameterizations of the nonlinear energy transfer in a gravity-wave spectrum. Part I: A new method for efficient computations of the exact nonlinear transfer integral, Journal of Physical Oceanography, 15, 1369–1377, 1985.

35 Holland, K. T. and Holman, R. A.: The statistical distribution of swash maxima on natural beaches, Journal of Geophysical Research: Oceans, 98, 10 271–10 278, 1993.

Holland, K. T. and Holman, R. A.: Video estimation of foreshore topography using trinocular stereo, Journal of Coastal Research, pp. 81–87, 1997.

Holman, R.: Extreme value statistics for wave run-up on a natural beach, Coastal Engineering, 9, 527–544, 1986.

Holman, R., Lippmann, T., O'neill, P., and Hathaway, K.: Video estimation of subaerial beach profiles, Marine Geology, 97, 225–231, 1991.

Hubbard, M. E. and Dodd, N.: A 2D numerical model of wave run-up and overtopping, Coastal Engineering, 47, 1–26, 2002.

Huisman, C. E., Bryan, K. R., Coco, G., and Ruessink, B.: The use of video imagery to analyse groundwater and shoreline dynamics on a dissipative beach, Continental shelf research, 31, 1728–1738, 2011.

Hunt, I. A.: Design of sea-walls and breakwaters, Transactions of the American Society of Civil Engineers, 126, 542–570, 1959.

Jennings, R. and Shulmeister, J.: A field based classification scheme for gravel beaches, Marine Geology, 186, 211–228, 2002.

Johannessen, O. and Bjorgo, E.: Wind energy mapping of coastal zones by synthetic aperture radar (SAR) for siting potential windmill locations, International Journal of Remote Sensing, 21, 1781–1786, 2000.

Leonard, B. P.: A stable and accurate convective modelling procedure based on quadratic upstream interpolation, Computer methods in applied mechanics and engineering, 19, 59–98, 1979.

Lippmann, T. C. and Holman, R. A.: Quantification of sand bar morphology: A video technique based on wave dissipation, Journal of Geophysical Research: Oceans, 94, 995–1011, 1989.

Mase, H.: Random wave runup height on gentle slope, Journal of Waterway, Port, Coastal, and Ocean Engineering, 115, 649–661, 1989.

Melby, J., Caraballo-Nadal, N., and Kobayashi, N.: Wave runup prediction for flood mapping, Coastal Engineering Proceedings, 1, 79, 2012.

Mentaschi, L., Besio, G., Cassola, F., and Mazzino, A.: Developing and validating a forecast/hindcast system for the Mediterranean Sea, Journal of Coastal Research, 65, 1551–1556, 2013.

Montella, R., Giunta, G., and Riccio, A.: Using grid computing based components in on demand environmental data delivery, in: Proceedings of the second workshop on Use of P2P, GRID and agents for the development of content networks, pp. 81–86, ACM, 2007.

Montella, R., Agrillo, G., Mastrangelo, D., and Menna, M.: A globus toolkit 4 based instrument service for environmental data acquisition and distribution, in: Proceedings of the third international workshop on Use of P2P, grid and agents for the development of content networks, pp. 21–28, ACM, 2008.

Montella, R., Giunta, G., Laccetti, G., Lapegna, M., Palmieri, C., Ferraro, C., and Pelliccia, V.: Virtualizing CUDA Enabled GPGPUs on ARM Clusters., in: PPAM (2), pp. 3–14, 2015.

Nunziata, F., Buono, A., Migliaccio, M., and Benassai, G.: Dual-polarimetric C-and X-band SAR data for coastline extraction, IEEE Journal of Selected Topics in Applied Earth Observations and Remote Sensing, 9, 4921–4928, 2016.

Ojeda, E., Ruessink, B., and Guillen, J.: Morphodynamic response of a two-barred beach to a shoreface nourishment, Coastal Engineering, 55, 1185–1196, 2008.

Paprotny, D., Andrzejewski, P., Terefenko, P., and Furmańczyk, K.: Application of empirical wave run-up formulas to the Polish Baltic Sea coast, PloS one, 9, e105 437, 2014.

Pham, Q., Malik, T., Foster, I. T., Di Lauro, R., and Montella, R.: SOLE: Linking Research Papers with Science Objects., in: IPAW, pp. 203–208, Springer, 2012.

Poate, T. G., McCall, R. T., and Masselink, G.: A new parameterisation for runup on gravel beaches, Coastal Engineering, 117, 176–190, 2016.

Reale, F., Dentale, F., Carratelli, E. P., and Torrisi, L.: Remote sensing of small-scale storm variations in coastal seas, Journal of Coastal Research, 30, 130–141, 2014.

Ruggiero, P., Holman, R. A., and Beach, R.: Wave run-up on a high-energy dissipative beach, Journal of Geophysical Research: Oceans, 109, 2004.

Rusu, L., Bernardino, M., and Guedes Soares, C.: Wind and wave modelling in the Black Sea, Journal of Operational Oceanography, 7, 5–20, 2014.

Senechal, N., Coco, G., Bryan, K. R., and Holman, R. A.: Wave runup during extreme storm conditions, Journal of Geophysical Research: Oceans, 116, 2011.

5 Shore Protection Manual, .: Department of the Army, Waterways Experiment Station, Corps of Engineers, Coastal Engineering Researcher Center, 2, 1984.

Skamarock, W. C., Klemp, J. B., and Dudhia, J.: Prototypes for the WRF (Weather Research and Forecasting) model, in: Preprints, Ninth Conf. Mesoscale Processes, J11–J15, Amer. Meteorol. Soc., Fort Lauderdale, FL, 2001.

Stockdon, H. F., Holman, R. A., Howd, P. A., and Sallenger, A. H.: Empirical parameterization of setup, swash, and runup, Coastal engineer-
10 ing, 53, 573–588, 2006.

Stockdon, H. F., Sallenger, A. H., Holman, R. A., and Howd, P. A.: A simple model for the spatially-variable coastal response to hurricanes, Marine Geology, 238, 1 – 20, 2007.

Stockdon, K. S. D. H. F., Sopkin, D. S. T. K. S., and Sallenger, N. G. P. A. H.: National assessment of hurricane-induced coastal erosion hazards: Gulf of Mexico, 2012.

15 Takewaka, S. and Nakamura, T.: Surf zone imaging with a moored video system, in: Proceedings of the International Conference on Coastal Engineering 2000, pp. 1211–1216, ASCE, 2001.

Tolman, H. L.: Effects of numerics on the physics in a third-generation wind-wave model, Journal of physical Oceanography, 22, 1095–1111, 1992.

Tolman, H. L.: Alleviating the garden sprinkler effect in wind wave models, Ocean Modelling, 4, 269–289, 2002.

20 Tolman, H. L. and Chalikov, D.: Source terms in a third-generation wind wave model, Journal of Physical Oceanography, 26, 2497–2518, 1996.

Tolman, H. L. et al.: User manual and system documentation of WAVEWATCH III TM version 3.14, Technical note, MMAB Contribution, 276, 220, 2009.

van der Meer, J., Allsop, N., Bruce, T., De Rouck, J., Kortenhaus, A., Pullen, T., Schüttrumpf, H., Troch, P., and Zanuttigh, B.: EurOtop:
25 Manual on wave overtopping of sea defences and related sturctures-An overtopping manual largely based on European research, but for worlwide application, 2016.

Vousdoukas, M. I., Almeida, L. P. M., and Ferreira, Ó.: Beach erosion and recovery during consecutive storms at a steep-sloping, meso-tidal beach, Earth Surface Processes and Landforms, 37, 583–593, 2012.

Wahle, K., Staneva, J., Koch, W., Fenoglio-Marc, L., Ho-Hagemann, H. T., and Stanev, E. V.: An atmosphere–wave regional coupled model:
30 improving predictions of wave heights and surface winds in the southern North Sea, Ocean Science, 13, 289, 2017.

Zhang, S. and Zhang, C.: Application of ridgelet transform to wave direction estimation, in: Image and Signal Processing, 2008. CISP'08. Congress on, vol. 2, pp. 690–693, IEEE, 2008.